Localization and Mobility of Gelsolin in Cells

John A. Cooper, David J. Loftus, Carl Frieden, Joseph Bryan,* and Eliot L. Elson

Departments of Biological Chemistry, Pathology, and Cell Biology and Physiology, Washington University School of Medicine, St. Louis Missouri 63110; and *Department of Cell Biology, Baylor College of Medicine, Houston, Texas

Abstract. To investigate the physiologic role of gelsolin in cells, we have studied the location and mobility of gelsolin in a mouse fibroblast cell line (C3H). Gelsolin was localized by immunofluorescence of fixed and permeabilized cells and by fluorescent analog cytochemistry of living cells and cells that were fixed and/or permeabilized. Overall, the images show that in living cells gelsolin has a diffuse cytoplasmic distribution, but in fixed cells a minor fraction is associated with regions of the cell that are rich in actin filaments. The latter fraction is more prominent after permeabilization of the fixed cells because some diffuse gelsolin is not fixed and is therefore lost during permeabilization, confirmed by immunoblots.

To determine quantitatively whether gelsolin is

bound to actin filaments in living cells, we measured the mobility of microinjected fluorescent gelsolin by fluorescence photobleaching recovery. Gelsolin is fully mobile with a diffusion coefficient similar to that of control proteins. As a positive control, fluorescent phalloidin, which binds actin filaments, is totally immobile. These results are supported by immunoblots on cells permeabilized with detergent. All the endogenous gelsolin is extracted, and the half-time for the extraction is ~5 s, which is about the rate predicted for diffusion. Therefore, gelsolin is not tightly bound to actin filaments in cells. The most likely interpretation of the difference between living and fixed cells is that fixation traps a fraction of gelsolin that is associated with actin filaments in short-lived complexes.

GELSOLIN is a Ca^{++}-dependent actin-binding protein that caps and severs actin filaments and binds to actin monomers to nucleate filament formation (for reviews see references 19 and 24). Gelsolin is found in the cytoplasm of a wide variety of mammalian cells (32) and is secreted by various cells (17). A single gene codes for two different mRNA's that specify the cytoplasmic and plasma forms (16). Because of our interest in cell motility and actin polymerization we would like to determine what role cytoplasmic gelsolin plays in cells. In a previous set of experiments we found that microinjection of gelsolin, which requires ~1 μM Ca^{++} for activity, has no detectable effects on cells, but microinjection of 40NT,[1] a proteolytic fragment of gelsolin, which is active in the absence of Ca^{++} (4), has dramatic effects (8). This difference is most likely due to the low concentration of Ca^{++} in cytoplasm, but may also be due to the presence of another molecule that inhibits gelsolin.

Previous studies on the localization of gelsolin in cells by

immunofluorescence have given conflicting results. In some cases, gelsolin was associated with actin-containing structures (20, 29, 32), but in other cases gelsolin had a diffuse distribution with little staining (5). Our previous microinjection results (8) predict that gelsolin should not bind to actin filaments. Therefore, to extend our previous studies and address this controversy, we both repeated the immunofluorescence localization of gelsolin in our system and localized gelsolin by a different technique, fluorescent analog cytochemistry, which involves microinjecting cells with fluorescent-labeled gelsolin and recording fluorescence images (26, 27). Fluorescence photobleaching recovery was used to determine quantitatively the mobility of fluorescent gelsolin microinjected into cells. Since actin filaments are immobile on short time scales, gelsolin bound to actin filaments should also be immobile.

Materials and Methods

Unless stated otherwise, biochemicals, immunochemicals, and column resins were from Sigma Chemical Co. (St. Louis, MO) and solvents and supplies were from VWR Scientific (Chicago, IL).

Preparation and Fluorescent Labeling of Proteins for Microinjection

Rabbit and mouse plasma gelsolin (8) and human platelet gelsolin (14) were prepared as described previously. An extra step of chromatography on

---

1. The name 40NT indicates that the fragment is from the NH_2-terminal half of the molecule and has an M_r of 40 kD, based on a new scheme for naming the fragments (Bryan, J. 1987. manuscript submitted for publication). This fragment was called CT40 in previous reports (4, 8) because it was derived from chymotrypsin. This fragment is similar to a thermolysin fragment called TL45n (6).

Sephacryl S-400 in 0.1 M NaCl, 1 mM EDTA, 10 mM Tris/HCl, 1.5 mM NaN$_3$, pH 8.0, was necessary in the preparation of rabbit plasma gelsolin for fluorescent labeling. This step removed trace amounts of high molecular weight contaminants that label more effectively than gelsolin. To couple lissamine-rhodamine B sulfonyl chloride (LRB-SC,[2] Molecular Probes, Eugene, OR) to gelsolin, the method of Sanger et al. (21) was modified slightly. We added 50 μg LRB-SC per mg gelsolin in 0.1 M NaCl, 0.1 M NaHCO$_3$, pH 9.0, and rotated the mixture overnight at 4°C. The reaction was quenched with 10 mM ethanolamine, and the mixture was gel-filtered on Sephadex G-25 and dialyzed into 150 mM KCl, 2 mM morpholino propane sulfonic acid (MOPS), pH 7.0, to remove free dye. To check for free dye and assess how well contaminants were labeled, the preparation was subjected to electrophoresis on an SDS–polyacrylamide gel, and rhodamine fluorescence was visualized. We found that LRB has λ_{max} = 570 nm with E = 77,000 M^{-1}cm^{-1}, by recording the visible spectrum of a known concentration of LRB-SC that had been reacted with excess ethanolamine at pH 10 and then adjusted to pH 7. The absorbance spectrum of LRB-rabbit plasma gelsolin showed a slight red shift with λ_{max} = 575 nm. Using these data to calculate the LRB concentration and the Bradford assay (3) (with rabbit skeletal muscle actin as the standard) to calculate the protein concentration, we found a dye to protein molar ratio of 0.7 to 1.1 for several preparations of LRB-rabbit plasma gelsolin. The dye to protein ratio was not measured for LRB-human platelet gelsolin, because a sufficient quantity was not available.

The functional activity of each of the preparations of LRB-labeled gelsolin was tested in two assays: the low shear viscometry of actin filaments (18) and the nucleation of actin polymerization from monomers, detected by pyrene actin fluorescence (9). The effect of gelsolin in the assays is to decrease the viscosity of actin filaments and increase the maximal rate of polymerization, respectively. The conditions were 0.1 M KCl, 2 mM MgCl$_2$, 0.1 mM CaCl$_2$, 10 mM imidazole pH 7.0, 20°C with rabbit skeletal muscle actin at 10 μM and 4 μM, respectively. Preparations of LRB-labeled rabbit plasma gelsolin and human platelet gelsolin had 70–130% of activity compared with unlabeled proteins, values that are consistent with 100% considering the errors in the assays and the protein measurements.

Commercial FITC-conjugated dog serum albumin was dialyzed and chromatographed on Sephadex G-25 to remove free dye. The dye concentration was measured spectrophotometrically with E$_{494}$ = 75,000 M^{-1}cm^{-1}, and the protein concentration was measured by the Bradford assay (3) with BSA as the standard. The dye to protein molar ratio was 25.

Microinjection and Imaging

A mouse fibroblast cultured cell line (C3H/10T1/2, ATCC CCL 226) was obtained from American Type Culture Collection (Rockville, MD) and maintained as described (8). Cells at sparse density on glass coverslips were microinjected and imaged as described (8) except that injection needles were backloaded with a glass capillary, as suggested by Dr. Yu-Li Wang (Worcester Foundation, Shrewsbury, MA). Proteins were dialyzed into 150 mM KCl, 2 mM MOPS, pH 7.0, for microinjection. Solutions were microfuged for 10 min before use. The LRB-gelsolin (plasma and cytoplasmic) concentration in the microinjection needle was 10 μM. To microinject rhodamine-phalloidin, a 3.3 μM stock in methanol (Molecular Probes, Eugene, OR) was dried down and redissolved at 33 μM in injection buffer. Cells microinjected with rhodamine–phalloidin showed no changes in shape or ruffling activity as also found by Wang (30). After microinjection, cells were incubated for varied periods of time (30 min to 2 h) to recover and allow incorporation of the fluorescent probe.

Fluorescence Photobleaching Recovery: Experimental Technique

Fluorescence photobleaching recovery (FPR) was performed as described (1) with the 514.5-nm line of an argon ion laser (Model 164, Spectra-Physics, Mountain View, CA) operating at 400 mW. A new modification of the system is the addition of two quarter wave plates between the laser and the first beam-splitting mirror. Rotation of these plates allows for a variable reduction in the intensity of the monitor phase beam (to reduce monitor phase bleaching) with no change in intensity of the bleach beam. A Dage ISIT video camera was attached to the microscope, allowing the collection of phase contrast and fluorescence images of cells that were bleached. The ob-

---

2. *Abbreviations used in this paper*: FPR, fluorescence photobleaching recovery; LRB-SC, lissamine-rhodamine B sulfonyl chloride.

jective was a Zeiss 100× Neofluor Ph3 NA 1.3 with spot radius 0.75 μm. Cells on coverslips were maintained in sealed chambers at 37°C in complete culture medium with 25 mM Hepes. The location of bleaching in cells was selected so that the spot size was small compared with the area of surrounding cytoplasm, to minimize the possibility that geometric factors would limit recovery.

Fluorescence Photobleaching Recovery: Data Analysis

To determine the spot radius, ω, a digital image of the spot was recorded with the video camera, and the fluorescence intensities were fit to a Gaussian profile. Recovery curves were analyzed with a computer program that included an immobile fraction and a mobile fraction, X$_m$, with one recovery time, τ$_D$. The diffusion coefficient, D, was calculated from D = ω^2/4τ$_D$. The value for the spot radius was checked by performing FPR on a solution of LRB-BSA and calculating back from the known diffusion coefficient.

In each experiment, data were first collected from a number of separate spots within a cell or solution. Each spot was photobleached only once. These recovery curves were analyzed individually, and the sum of all these curves was also analyzed. If the mobile fraction was 100%, then subsequent spots were photobleached many times and the traces were summed to improve the signal-to-noise ratio. If the mobile fraction was less than 100%, then each subsequent spot was only photobleached once.

For experiments with cells, 5–20 spots were bleached per cell. The mobile fraction listed in Table I is the average of the mobile fraction from 33 spots for gelsolin, and 60 spots for phalloidin. The diffusion coefficient for gelsolin is based on 128 scans of 2 spots.

FPR data contains both systematic and random error. Systematic error includes the difference in recovery between different spots within one sample. While these differences should be small in a solution of a single substance, they may be large in actin filament solutions and cytoplasm, which are spatially heterogeneous. Since in these experiments the signal in a typical recovery curve from one spot was low, curves from different spots were added together for analysis, and spot-to-spot variation was lost. Therefore, our error analysis excludes this component, and the reported error is an underestimate to an uncertain degree. Random error includes the noise in the signal, which can be measured. To estimate the random error in the fitted values of X$_m$ and τ$_D$, a theoretical curve was generated using those given parameters. Random noise with a Gaussian distribution and proportional to the fluorescence intensity was added to the curve, in an quantity chosen to match that in the experimental record. The noisy theoretical curve was then fit to generate values of X$_m$ and τ$_D$. This procedure was repeated many times to generate standard deviations for X$_m$ and τ$_D$.

Antibodies against Gelsolin

A New Zealand White adult female rabbit was immunized with pure mouse plasma gelsolin, which was excised and electroeluted from SDS-polyacrylamide gels (13). The immunization and bleeding protocol was as described (11). For affinity-purified antibodies, mouse plasma gelsolin was coupled to CNBr-activated Sepharose. Antiserum was mixed with the resin for several hours and the column was washed with 100 vol of 0.3 M NaCl, 10 mM Tris, pH 8.0. Antibodies were eluted with 0.1 M glycine, pH 2.8, immediately neutralized with 1 M Tris, pH 8.5, and dialyzed into PBS (150 mM NaCl, 20 mM NaP$_i$, pH 7.5, 1.5 mM NaN$_3$). The yield of affinity-purified antibody was 130 μg per mL of antiserum.

Staining of Cells with Antibodies

Cells on glass coverslips were fixed with 1% (wt/vol) paraformaldehyde in PBS for 30 min and permeabilized with either −20°C acetone for 30 s, 0.1% (wt/vol) Triton X-100 for 5 min, or 0.1 mg/mL digitonin for 5 min. The cells were quenched with 10 mM ethanolamine in PBS and blocked with 10 mg/mL BSA in PBS. Cells were stained with 5 μg/mL affinity-purified rabbit anti-gelsolin antibodies in PBS with 10 mg/mL BSA for 1 h, rinsed with PBS 3 times for 10 min each, stained with rhodamine-labeled goat anti-rabbit immunoglobulin (Tago, Burlingame, CA) diluted 1:500 in PBS for 1 h, and rinsed with PBS 3 times for 10 min each. As a control, rabbit immunoglobulin at 5 μg/mL was substituted for the rabbit anti-gelsolin antibodies. When cells were also stained with NBD-phallacidin (Molecular Probes, Eugene, OR), 25 μl of 3.3 μM stock was used per coverslip. In experiments where cells were injected with anti-gelsolin antibodies, the staining with the first antibody was omitted from the procedure. Coverslips were mounted on slides in PBS with 1 mg/mL P-phenylenediamine and viewed on a Zeiss
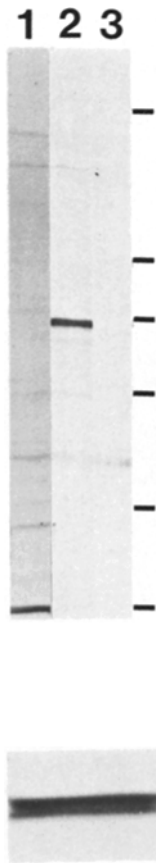
1 2 3

Figure 1. Immunoblots of whole cells. (*Upper panel*) Preparations of whole C3H cells were subjected to electrophoresis in one wide lane and blotted. Adjacent strips of the blot paper were stained. 1-Amido black, 2-Immune rabbit anti–mouse plasma gelsolin serum, 3-Preimmune serum from the same rabbit. Positions of molecular mass standards are indicated on the right. From top to bottom, they are 200, 116, 93, 67, and 45 kD, and the dye front. (*Lower panel*) A magnified view of the 90 K region from another immunoblot of the same sample used for the upper panel, also stained with immune serum. The 93- and 90-kD bands of plasma and cytoplasmic gelsolin, respectively, are resolved on this gel. In most immunoblots, including the one in the upper panel, they are not well resolved.

IM35 fluorescence microscope with a 100-W mercury arc and a 100× 1.3 NA phase contrast objective. For double label experiments with NBD or fluorescein and rhodamine, appropriate filters were used to exclude significant crossover. Also, the NBD image was photographed first, which bleached the NBD and ensured no crossover, which was especially important for comparisons of the distributions of actin filaments by NBD-phallacidin and gelsolin by rhodamine-antibodies. Kodak Tri-X film was used for photographing fluorescent specimens on the microscope, and Plus-X film was used for photographing the video monitor.

Immunoblots on Cell Extracts

Cells were grown to near confluence in 35-mm plastic dishes. For Triton solubilization, each dish was rinsed twice with PBS and received 0.75 mL of 0.1% (wt/vol) Triton X-100, 150 mM KCl, 5 mM MgCl₂, 1 mM EGTA, 10 mM imidazole/HCl, pH 7.0. After incubation with mixing for a specified time, the solution was removed from the dish and dialyzed against 2 mM Tris/HCl pH 8.0 for several hours. 0.25 mL of 4× SDS sample buffer was added, and the solution was boiled for 1 min. To prepare SDS-gel samples of either whole cells or the Triton-insoluble fraction, the dish was rinsed twice with PBS and 1 mL of 1× SDS sample buffer was added. The dish was carefully held in boiling water for 1 min with mixing. The solution was withdrawn and boiled for another minute.

Samples were run on 10% SDS-polyacrylamide gels (12) and blotted onto 0.22 μm nitrocellulose paper (28). The paper was blocked with BSA (10 mg/mL) in TTBS (0.05% (wt/vol) Tween-20, 0.3 M NaCl, 20 mM Tris/HCl, pH 7.5, 0.01% NaN₃) for 30 min. The paper was stained for several hours with rabbit anti–mouse plasma gelsolin (1:100 dilution of antiserum in TTBS, 0.22 μm filtered), rinsed with TTBS, stained for several hours with alkaline phosphatase-conjugated goat anti-rabbit IgG (1:200 dilution in TTBS) and rinsed with TTBS. The alkaline phosphatase was developed (10), and the paper was photographed with Polaroid Type 55 film and a yellow filter.

Results

Localization of Gelsolin by Immunofluorescence

Since a controversy exists over whether gelsolin is localized to actin filaments by immunofluorescence, we first prepared new antibodies and examined this question in our system. Polyclonal antibodies were prepared by immunizing rabbits with mouse plasma gelsolin. The antibodies are specific for gelsolin and recognize both plasma and cytoplasmic isoforms, shown by the presence of bands with apparent M_r of 93 and 90 kD, respectively, on immunoblots (Fig. 1). The intensity of the 90-kD band is about twice that of the 93 kD. If the antibodies bind to the two isoforms with a similar affinity and stoichiometry, which is probable since the primary protein structures are very similar (16), then cells contain about twice the amount of cytoplasmic gelsolin as plasma gelsolin. Affinity-purified antibodies were prepared and used to stain cells that were fixed with formaldehyde and permeabilized with cold acetone or detergent. Albumin was used to block nonspecific binding instead of serum proteins, which might contain plasma gelsolin and cause spurious results (5). The staining intensity was ample – it was readily observed by eye and photographed. The distribution of fluorescence partially coincides with that of stress fibers and cell edges, which are rich with actin filaments detected by double staining with fluorescent phalloidin (Figs. 2 and 3). The staining also has a component with a diffuse distribution, and other results (presented below) show that some of the diffuse component is not fixed by this procedure.

In addition, the fluorescence distribution has a granular component, seen in both the perinuclear and peripheral regions of the cell, which we initially thought may represent plasma gelsolin in secretory vesicles. However, permeabilizing only the plasma membrane (with cold acetone or digitonin) or all membranes (with Triton X-100) gives the same results (data not shown), which indicates that the granular component is not membrane-bound vesicles.

We considered that release of internal Ca^{++} during fixation might activate gelsolin, causing it to bind to actin filaments. To test this idea, 50 mM EGTA was included in the buffer used to rinse and fix the cells. The results were unchanged.

As an alternative method of using the antibodies to localize gelsolin, we microinjected affinity-purified antibodies into the cytoplasm of cells, and then fixed, permeabilized, and stained the cells with fluorescent goat anti–rabbit antibody (Fig. 4). The results are similar to those with the traditional approach above (Figs. 2 and 3), except that the diffuse component is more prominent. Much of the fluorescence is still in the form of small granules, most of which have no corresponding structure in the phase–contrast image. Plasma gelsolin in secretory vesicles should be unavailable to these antibodies, so the granular fluorescence may represent aggregates of cytoplasmic protein. When the concentration of antibody in the microinjection needle was varied from 1–25 μM, the results were similar. The antibodies never caused a global aggregation of gelsolin, and the antibodies had no effect on the shape and ruffling activity (observed by time-lapse video phase contrast microscopy) of the cells (data not shown).
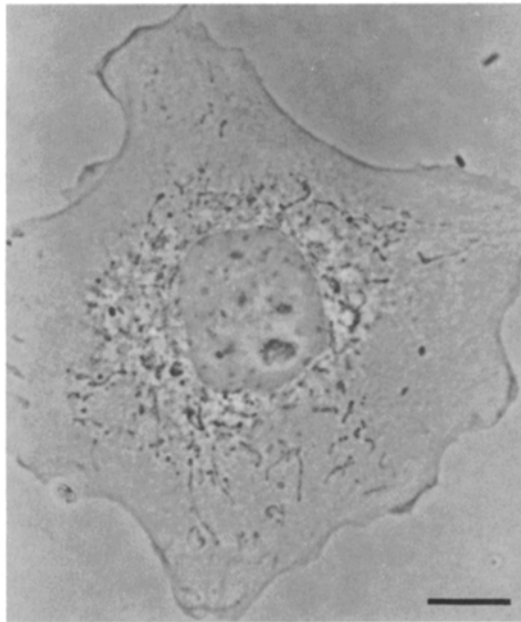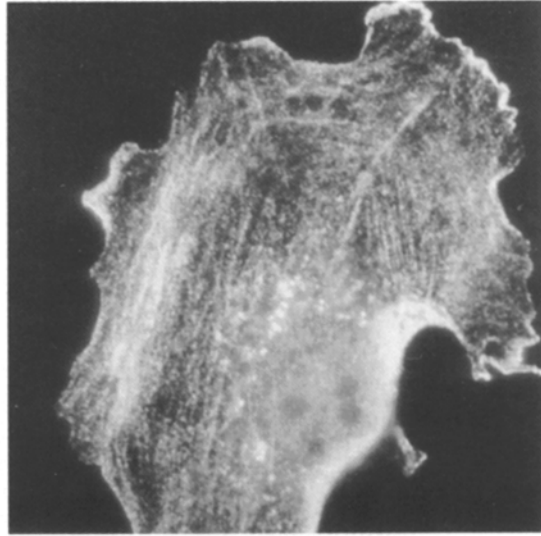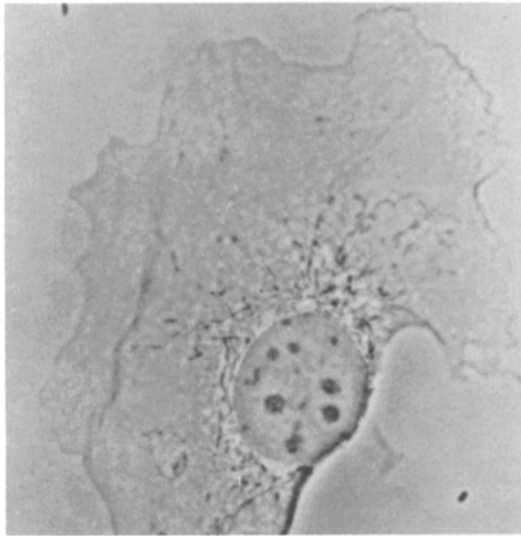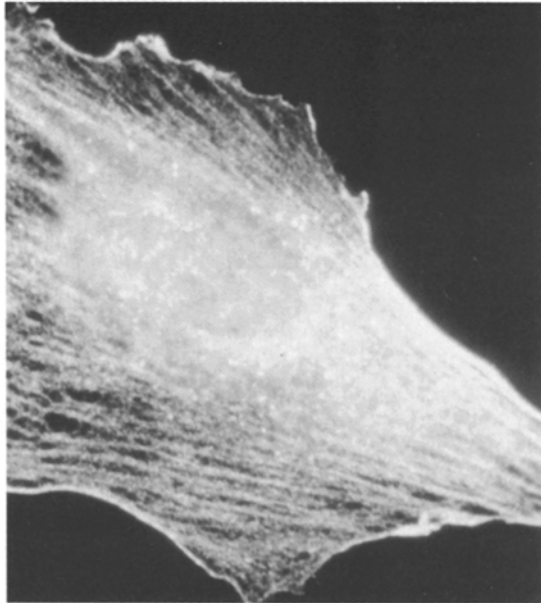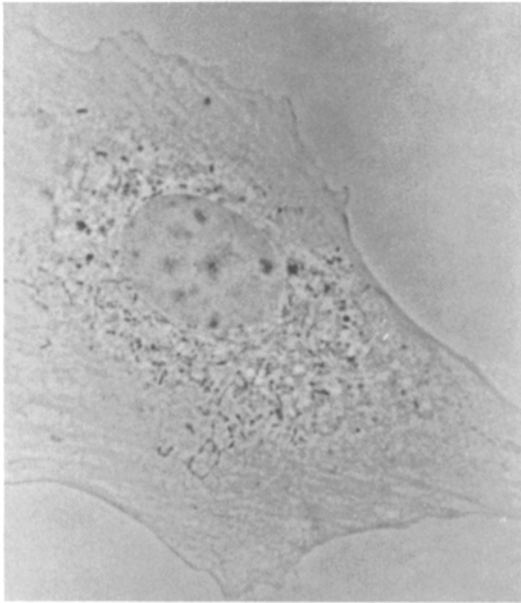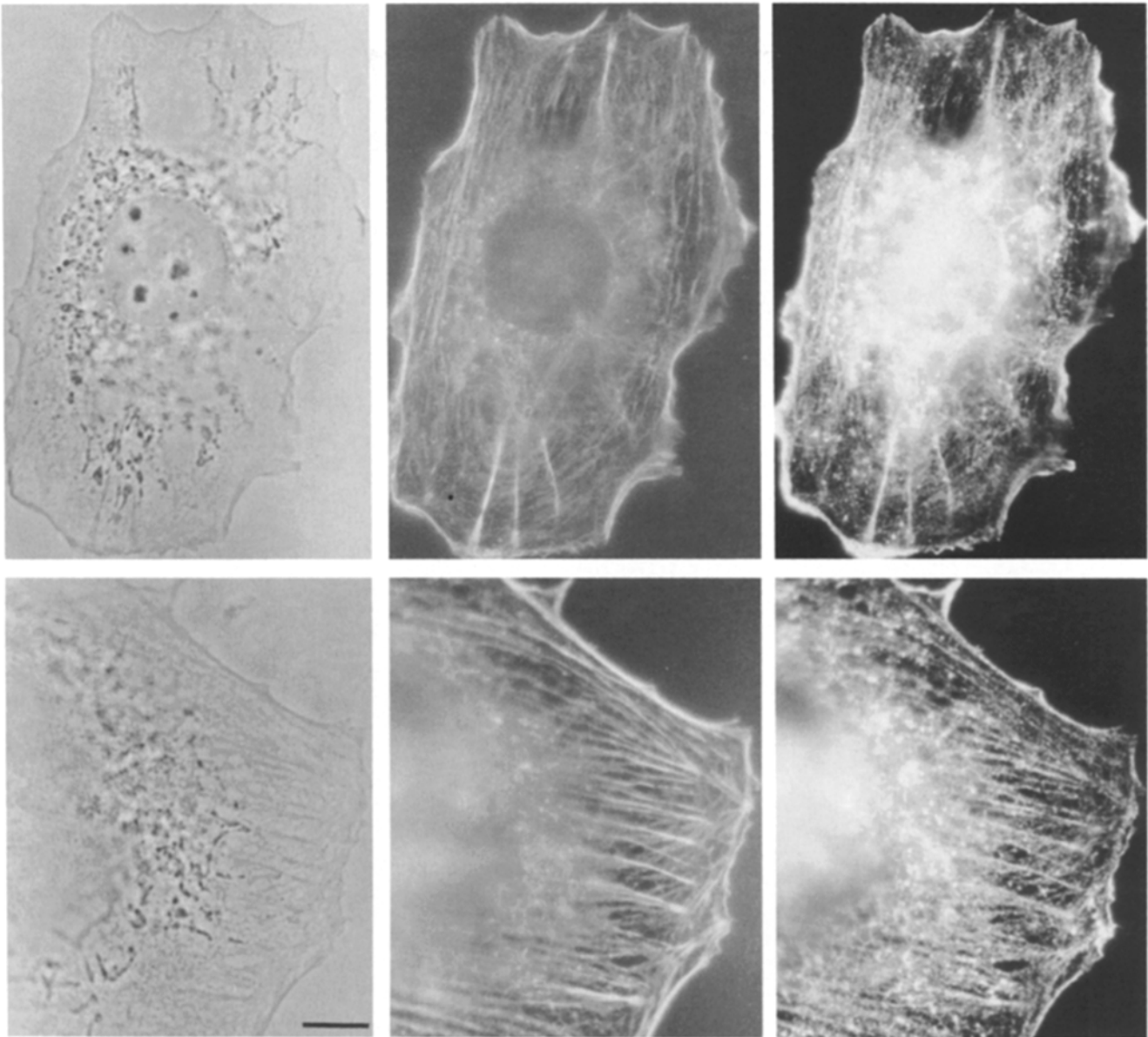
Figure 3. Cells stained with NBD-phallacidin and anti–gelsolin antibodies. Phase contrast (*left*), NBD fluorescence (*middle*), and rhodamine fluorescence (*right*) images of fibroblasts stained with both NBD-phallacidin and anti–gelsolin antibodies. Stress fibers and cell cortexes are fluorescent in both images. Bar, 10 μm.

Localization of Gelsolin by Fluorescent Analog Cytochemistry

Fluorescent analog cytochemistry was used as an alternative method of localizing cytoplasmic gelsolin. We prepared a fluorescent derivative of gelsolin, injected it into the cytoplasm of cells, and recorded fluorescent images of the cells. Both plasma and cytoplasmic (platelet) gelsolin were coupled to LRB. The preparations had no free dye, a dye to protein molar ratio of ∼1, and full activity (described in Materials and Methods).

The value of this method depends on the fluorescent gelsolin acting as a tracer for the endogenous gelsolin. The injected gelsolin must equilibrate with all the cellular pools. Therefore, we injected the minimum concentration of LRB-gelsolin necessary for visualization. The concentration in the microinjection needle was 5–10 μM. Since the injection volume is ∼10% (8), the cytoplasmic concentration was 0.5–1 μM, which is at the low end of range of the estimated endogenous concentration of gelsolin of 1–4 μM (23). Furthermore, the time between injection and imaging was varied from 15

Figure 2. Cells stained with anti–gelsolin antibodies. Phase contrast (*left*) and rhodamine fluorescence (*right*) of fibroblasts stained with affinity purified rabbit anti–gelsolin and rhodamine-conjugated goat anti–rabbit immunoglobulin antibodies. The bottom panel is a control where nonimmune immunoglobulins were substituted for anti–gelsolin. The exposure time and other photographic parameters were the same for all the fluorescence micrographs. Bar, 10 μm.
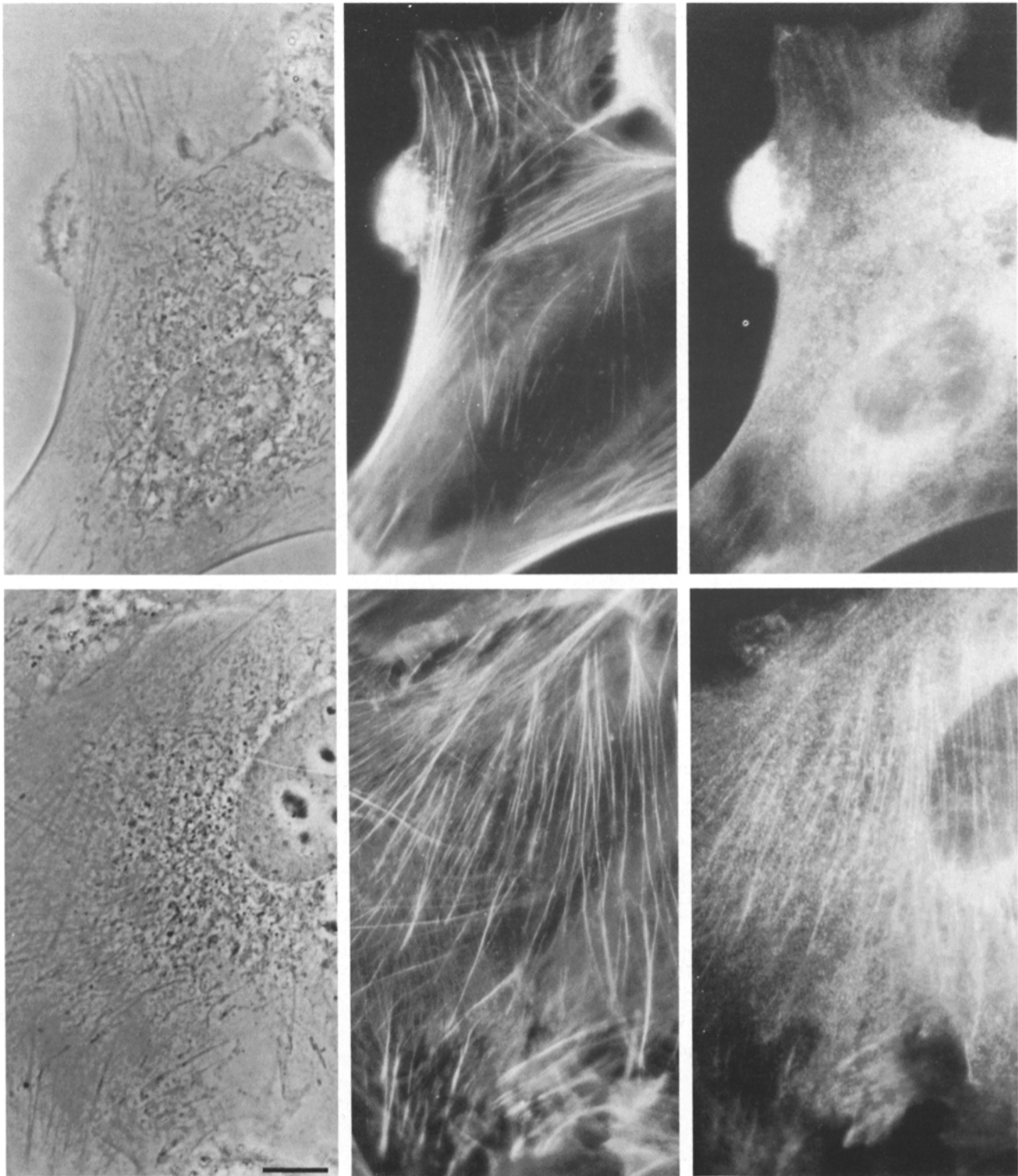
Figure 4. Cells microinjected with anti-gelsolin antibodies. Phase contrast (*left*), NBD fluorescence (*middle*), and rhodamine fluorescence (*right*) images of fibroblasts that were injected with affinity purified anti-gelsolin antibodies, and then fixed, permeabilized and stained with both NBD-phallacidin and rhodamine-labeled goat anti-rabbit immunoglobulin antibodies. The diffuse cytoplasmic component of the gelsolin stain is more prominent here than with the traditional immunofluorescence approach of Fig. 3. Lower amounts of injected antibody gave the same results. Bar, 10 μm.

min to 2 h with no change in results. Also, as another control to ensure mixing of injected and endogenous gelsolin, the injected cells were treated with cytochalasin D (2 μM, 60 min), which caused the cells to round up and lose their stress fibers and ruffles. Cytochalasin D was removed and the cells recovered for 90 min, during which time they re-spread and
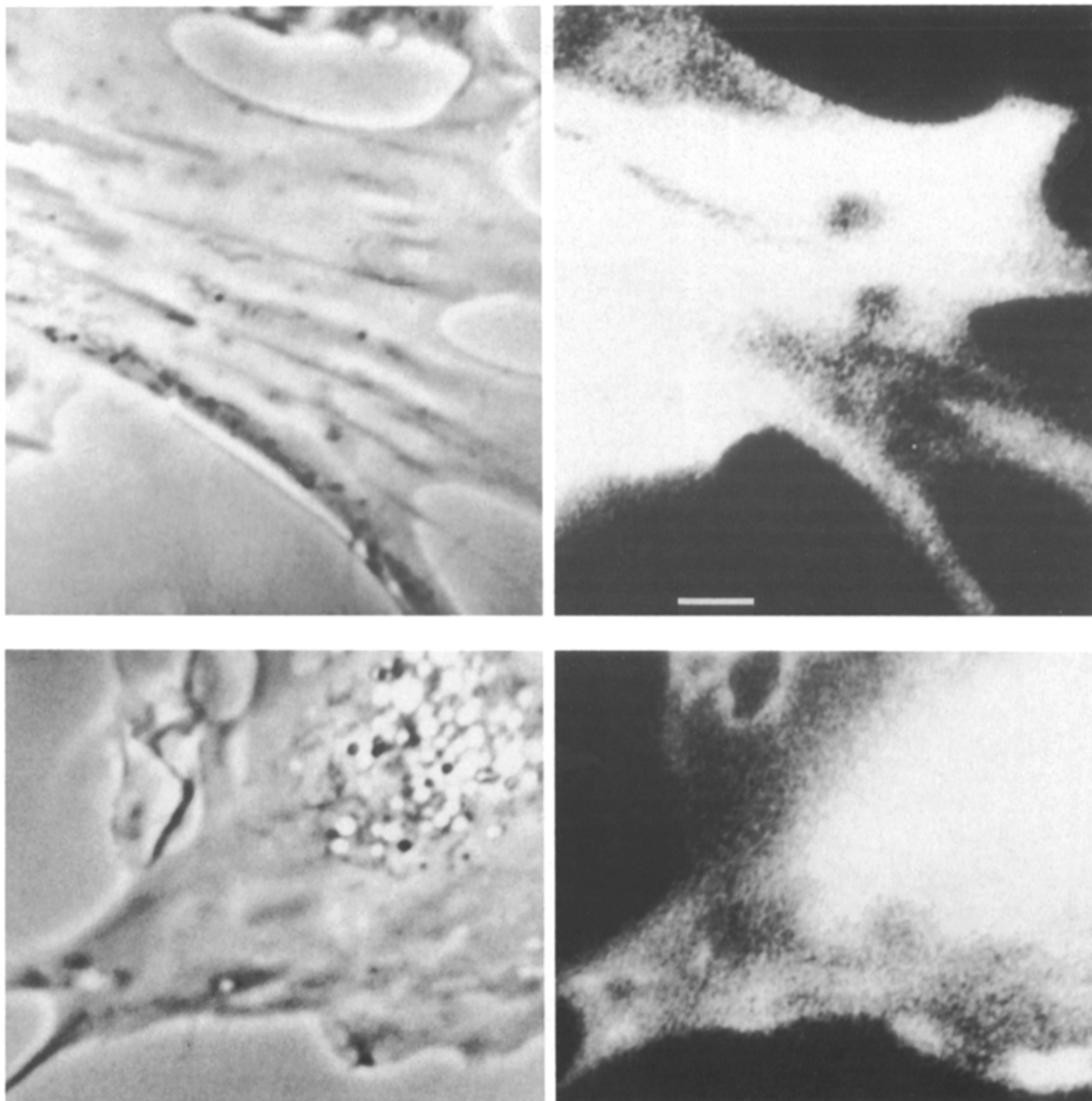
Figure 5. Living cells microinjected with LRB-Gelsolin. Phase contrast and fluorescence images. The distribution of fluorescence is homogeneous throughout the cytoplasm, without selective localization in stress fibers, ruffles or edges. Based on the phase contrast images, the cell in the upper panel has stress fibers, and the cell in the lower panel has ruffles. Also, fixing and staining a similar preparation of cells with fluorescent phalloidin shows that all cells contain stress fibers. These fluorescence images were collected with the video camera and underwent a large amount of contrast enhancement, to examine the peripheral regions where selective localization would be most noticeable. Therefore, the central regions are over-exposed. However, less contrast enhancement of the same images shows no stress fiber staining or other inhomogeneities in the central regions. Bar, 5 μm.

ruffles and stress fibers reformed. Again the results were unchanged. Also, the same results were obtained with plasma and cytoplasmic gelsolin.

Images of live cells show only a diffuse cytoplasmic distribution of gelsolin, without selective staining of stress fibers or ruffles (Fig. 5). These cells were subsequently fixed and stained with NBD-phallacidin to document that they did indeed have stress fibers and actin-rich cortexes and ruffles.

The diffuse distribution observed by fluorescent analog cytochemistry is strikingly different from that by immunofluorescence. To investigate this difference, we fixed, but did not permeabilize, cells that were injected with LRB–gelsolin. This protocol has the added advantage of occasionally creating blebs of plasma membrane, that should contain only soluble components of the cytoplasm but not large insoluble elements like stress fibers and organelles (22, 25, 31). In this
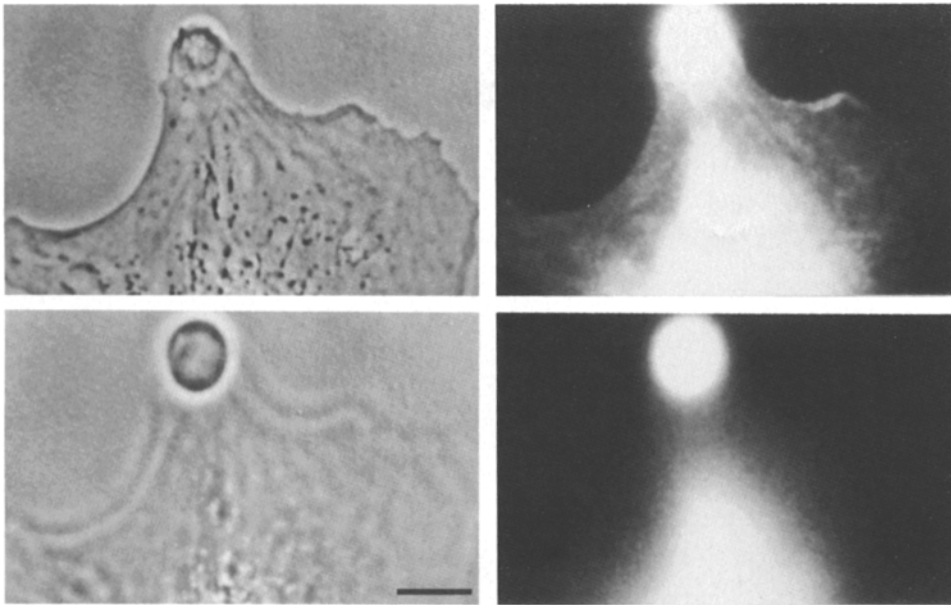
Figure 6. Two focal planes of a cell microinjected with LRB–gelsolin and fixed but not permeabilized. The upper panels (*left*, phase contrast; *right*, fluorescence) are images in which the bottom of the cell is in focus. A few linear structures, probably stress fibers, are present. The lower panels are from a higher plane and show a bleb, which was induced by the fixation procedure. The bleb, which should not contain actin filaments, is intensely fluorescent, which indicates that a large fraction of the gelsolin is free to diffuse away if the membrane is permeabilized. Bar, 10 μm.

case, some linear fluorescent structures are seen in the diffuse background of the cytoplasm, and the blebs are also fluorescent (Fig. 6). We were concerned that these linear structures might represent path-length artifacts. When FITC–albumin is co-injected along with LRB–gelsolin, to serve as an internal marker of a diffuse cytoplasmic distribution, the linear structures are present in the LRB-gelsolin, but not the FITC–albumin, image (Fig. 7). Other regions of the cell, such as ruffles and cell edges, which have a high concentration of actin filaments, also have a high concentration of
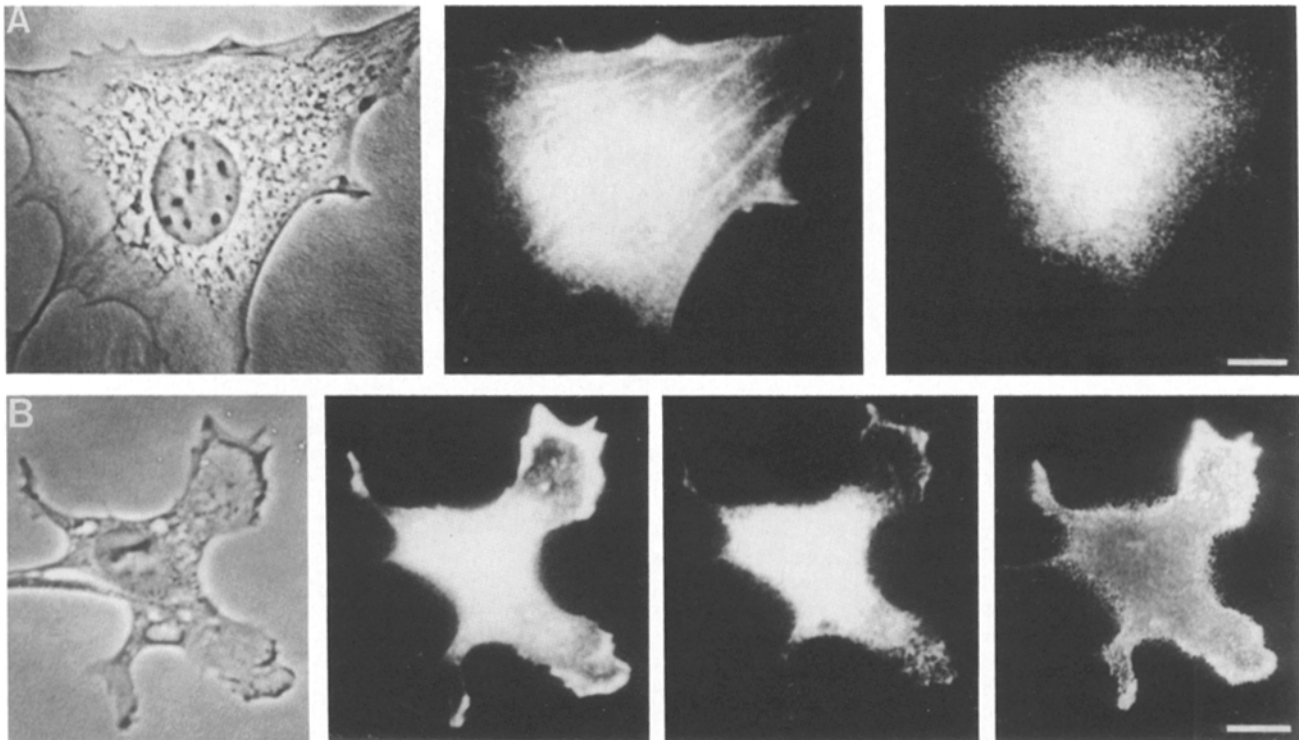

Figure 7. Cells microinjected with both LRB-gelsolin and FITC–albumin. These cells were fixed and permeabilized. In the upper panel, the images are phase contrast, rhodamine fluorescence, and fluorescein fluorescence (left to right). The LRB–gelsolin is present in linear structures that are not observed with FITC–albumin, a marker for cytoplasmic volume. In the lower panel, the images are also phase, rhodamine, and fluorescein (left to right) with the addition of a fourth image on the right, which is the ratio of the LRB-gelsolin image to the FITC–albumin image. These images show that gelsolin is concentrated at ruffles and cell edges, which are known to have high concentrations of actin filaments. Bar, 10 μm.
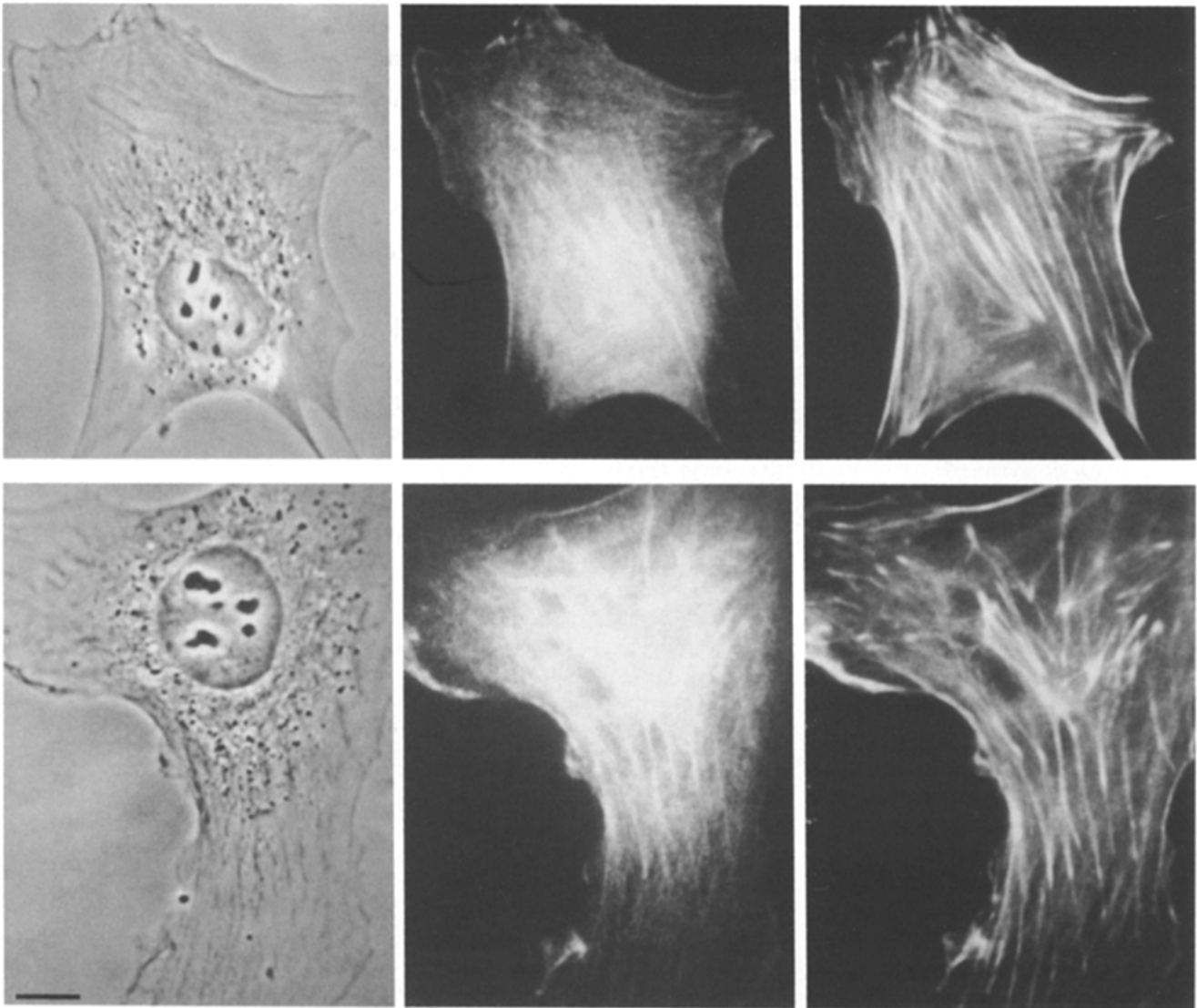
Figure 8. Cells microinjected with LRB–gelsolin and stained with NBD–phalloidin after fixation and permeabilization. The images are phase contrast, rhodamine fluorescence and NBD fluorescence (*left* to *right*). The linear structures in the gelsolin image correspond to stress fibers, shown in the phalloidin image. Cell ruffles and edges that are rich in actin filaments, shown in the phalloidin image, also show LRB-gelsolin fluorescence. Bar, 10 μm.

LRB–gelsolin, which is best shown by normalizing for path length (Fig. 7). When such cells are permeabilized after fixation, the actin filament staining pattern is even more prominent (Fig. 8). The blebs and their contents are no longer present, so the soluble diffuse component of gelsolin in the remainder of the cell must also have diffused away.

In injected cells undergoing mitosis, LRB–gelsolin has a diffuse distribution with exclusion from the chromosomes and spindle and no concentration in the contractile ring (data not shown).

Extraction of Gelsolin from Fixed Cells

Based on the above results, we considered the possibility that free gelsolin, with a diffuse cytoplasmic distribution, might be poorly fixed and therefore extracted by permeabilization before the antibody staining. Cells were fixed and extracted as usual, and gelsolin was measured in the extract by immu-

noblots (Fig. 9). Only about half of the gelsolin is fixed by this protocol. The fixation slightly increases the mobility of the gelsolin on SDS–PAGE, presumably due to internal crosslinks, which is also seen with cell samples that were fixed after extraction (Fig. 9).

Extraction of Gelsolin from Living Cells

To explain the difference between the results with live vs. fixed cells, we asked whether gelsolin was bound to actin filaments in live cells, despite the absence of specific localization in the fluorescence images. We were surprised to observe that any gelsolin was associated with actin filaments in fixed cells and wanted to search carefully for such an interaction in living cells. As a first step, we determined that LRB–gelsolin does not remain associated with stress fibers after permeabilization with detergent. Cells were injected with LRB–cytoplasmic gelsolin and permeabilized with Triton
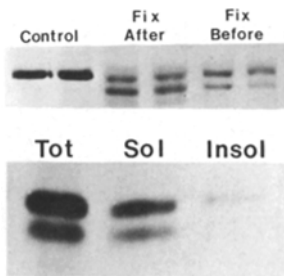
Figure 9. Triton solubilization of gelsolin from cells fixed with formaldehyde. Both panels show the gelsolin region of immuno-blots of cell extracts stained with anti-gelsolin. (*Upper panel*) Control experiment to show the effect of formaldehyde on gelsolin. The lanes marked Control are from cells that were not fixed. The lanes marked *Fix After* are Triton extracts, in which gelsolin is soluble, that were treated with formaldehyde. These lanes, compared with control, show that formaldehyde causes gelsolin to run as two bands with higher mobility. The lanes marked *Fixed Before* are whole cells fixed with formaldehyde. These lanes, compared with *Fix After*, show that the gelsolin band again splits into two bands of higher mobility and that slightly less gelsolin is extracted. This small amount was not visualized as a new band of lower mobility and presumably was not soluble or did not electrophorese. (*Lower panel*) Triton solubilization of gelsolin from fixed cells. The lanes are *Total*, *Soluble*, and *Insoluble*. The soluble fraction of gelsolin is greater than the insoluble. These cells were fixed with formaldehyde and permeabilized with Triton in a protocol identical to that used for immunofluorescence. Therefore, the immunofluorescence images only reflect a subset of the gelsolin. The sum of the soluble and insoluble gelsolin appears less than the total. This difference is consistent and may represent nonlinearity of the immunoblots.
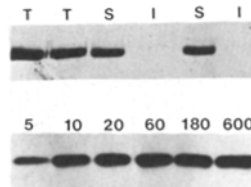

Figure 10. Triton solubilization of gelsolin from living cells. Both panels show the gelsolin region of immunoblots of cell extracts. (*Upper panel*) T, total cell; S, soluble in Triton; I, insoluble in Triton. The results show that all the endogenous gelsolin is soluble. These cells were extracted with Triton for 30 min. The panel includes duplicates, with two Ts and two pairs of Ss and Is. A single pair of S and I is derived from one group of cells. (*Lower panel*) Time course of gelsolin solubilization. Cells were extracted with Triton for times indicated in seconds above the lanes. The soluble portion was applied to the gel. All the gelsolin is extracted in 10 s.

under conditions that preserve many actin filaments (0.1% Triton X-100, 150 mM KCl, 5 mM $MgCl_2$, 0.5 mM EGTA, 5 mM MOPS, pH 7.0 for 30 min). No fluorescence remains with the cell preparations (data not shown).

We considered the possibility that endogenous gelsolin might be tightly bound to filaments by a mechanism in which the LRB–gelsolin could not participate or that required a longer period of time than the recovery time allowed to the injected cells. Therefore, the ability of detergent to extract endogenous gelsolin was measured, using immunoblots. All of the gelsolin is extracted, and the half-time for extraction is ∼5 s, a value consistent with the rate of diffusion out of the cell (Fig. 10).[3] Also, when these Triton-permeabilized cells (cytoskeletons) were subsequently fixed and stained with anti-gelsolin antibodies, no fluorescent staining was observed (data not shown).

Mobility of Gelsolin by Fluorescence Photobleaching Recovery

To assess the interaction of gelsolin with actin filaments in a more quantitative manner, we measured the mobility of fluorescent gelsolin in living cells by fluorescence photobleaching recovery (Table I). The recovery was complete (mobile fraction 97%), and the diffusion coefficient was 3.0 × 10^{-8} cm^{2}s^{-1}. Cells were microinjected with LRB–gelsolin and allowed to recover for 1–4 h. Fluorescent cells were bleached in peripheral areas, which were free of vesicles and were certain to contain actin filaments, including stress fibers. When stress fibers were visible in the phase contrast image, we selected spots on the stress fibers for bleaching.

However, even when stress fibers were not seen in the phase contrast image, subsequent staining with NBD-phallacidin showed that these regions had many small stress fibers and photobleaching with rhodamine-phalloidin (presented below) showed that immobile actin filaments were present. To improve the signal, from 5 to 15 different spots were bleached in each cell, and the recovery curves were summed.

Rhodamine phalloidin, which binds tightly to actin filaments (7), was used as a positive control, suggested by the studies of Wang (30). The mobile fraction in the summed recovery curves was 2% (Table I). The largest mobile fraction for a single curve was 20%. The diffusion coefficient in this case is not measurable. Compared with LRB-gelsolin, the same parameters were used for the bleaching, but the fluorescence levels were two- to fivefold higher.

Discussion

We are interested in the physiologic role of gelsolin in cells. Our previous studies (8) found that microinjected gelsolin is not active in cells, but 40NT, a proteolytic fragment of gelsolin that is active without Ca^{++}, has dramatic effects. Therefore, we expected that microinjected gelsolin would be free in the cytoplasm and would not bind to actin filaments. The data in this paper confirm this prediction. Fluorescence images of living cells injected with fluorescent-labeled gelsolin show only a diffuse cytoplasmic distribution. Areas of cells rich in actin filaments are not selectively stained. Also, FPR shows that gelsolin is fully mobile even though actin filaments are totally immobile.

The FPR experiments do not rule out the existence of a

Table I. Fluorescence Photobleaching Recovery in Living Cells

	Mobile fraction	Diffusion coefficient
	%	$(10^{-8}\ cm^2s^{-1})$
Gelsolin	97 ± 4	3.0 ± 0.4
Phalloidin	2 ± 2	Not available

The values for the error represents 1 SD and were calculated as described in the Materials and Methods section. As discussed more fully there, the error values may be underestimates. This parameter cannot be measured because the mobile fraction is so low. The diffusion coefficient of gelsolin in solution is 65 × 10^{-8}cm^{2}s^{-1} (23). In cytoplasm the diffusion coefficient of several control proteins with M_r ranging from 12,000–440,000 is 0.9–1.7 × 10^{-8}cm^{2}s^{-1} (15).

---

3. Gelsolin, with a diffusion coefficient of 3.0 × 10^{-8}cm^{2}s^{-1} (Table I), should diffuse out of a cell 10-μm thick in a time of 8 s, based on $t = \omega^2/4D$.

small gelsolin–actin complex. In cytoplasm, proteins of widely varying sizes diffuse at the same slow rate due to unknown interactions (2, 15). Hence, if gelsolin were bound to an actin oligomer or a short actin filament that was not otherwise immobilized, the diffusion coefficient might be the same as that of free gelsolin. The FPR data also do not exclude the existence of a short-lived complex of gelsolin with immobile actin filaments, an idea that is presented below as a possible explanation for some other results. If the affinity were low and the exchange rate for binding of gelsolin to actin filaments were high compared with the rate of diffusion, then the bound component would not be observed experimentally.

These localization results, performed by fluorescent analog cytochemistry, are at odds with other results localizing gelsolin by immunofluorescence. In those experiments, gelsolin was found in stress fibers, cell edges, and attachment sites of transformed fibroblasts (29), in cortical cytoplasm adjacent to particles being phagocytized by macrophages (32), in the terminal web region of intestinal epithelial cells (32), and in the I-band and subsarcolemmal region of striated muscle (20, 32). All these sites are rich in actin filaments, suggesting that gelsolin binds to actin filaments. On the other hand, a subsequent set of immunofluorescence experiments found no staining of stress fibers or I-bands and suggested that the staining in prior experiments was due to plasma gelsolin in the antibody preparations (5).

We also localized gelsolin by the immunofluorescence approach in our system, preparing new affinity-purified polyclonal antibodies of high titer and specificity. Stress fibers, ruffles and cell edges are selectively stained; this distribution coincides with that of actin filaments. Chelating Ca^{++} had no effect on this result, so gelsolin is probably not being activated by release of internal Ca^{++} during fixation. In addition, the gelsolin distribution also has a granular cytoplasmic component, which is not due to membrane-bound vesicles, shown by selective permeabilization and antibody injection.

Several factors contribute to the disparity between the results from fluorescent analog cytochemistry and immunofluorescence. The appearance of the actin filament staining pattern in cells microinjected with fluorescent gelsolin and then fixed indicates that fixation induces binding of gelsolin to actin filaments. Perhaps a low affinity, short-lived complex of gelsolin with actin filaments, which is present in undetectably small amounts in live cells, is trapped by fixation. This interaction may correlate with the in vitro activity of 26NT, a gelsolin fragment that binds along the sides filaments with a K_d of ~2.5 μM, has no severing activity, and does not require Ca^{++} (Bryan, J., 1987, manuscript submitted for publication). Also, the diffuse component of gelsolin, which is presumably free, may be poorly fixed and therefore lost on permeabilization. Two experiments support this idea. Fixed cells can have blebs of plasma membrane, which contain soluble cytoplasmic components (22, 25, 31). Microinjected fluorescent gelsolin fills these blebs, which disappear upon permeabilization. Also, immunoblots of cells before and after fixation and permeabilization show that a moderate amount of endogenous cellular gelsolin is lost. We have also observed this phenomenon with fluorescent proteins used as tracers for microinjection—the fluorescence intensity of the fixed and permeabilized cell can be much less than that of the live cell.

References

1. Axelrod, D., D. E. Koppel, J. Schlessinger, E. Elson, and W. Webb. 1976. Mobility measurement by analysis of fluorescence photobleaching recovery. Biophys. J. 16:1055–1069.
2. Berg, O. 1986. Effective diffusion rate through a polymer network: influence of nonspecific binding and intersegment transfer. Biopolymers. 25:811–821.
3. Bradford, M. 1976. A rapid and sensitive method for the quantitation of microgram quantities of protein utilizing the principle of protein-dye binding. Anal. Biochem. 72:248–254.
4. Bryan, J., and S. Hwo. 1986. Definition of an N-terminal Actin-binding Domain and a C-terminal Ca^{2+} regulatory domain in human brevin. J. Cell Biol. 102:1439–1446.
5. Carron, C. P., S. Hwo, J. Dingus, D. M. Benson, I. Meza, and J. Bryan. 1986. A re-evaluation of cytoplasmic gelsolin localization. J. Cell Biol. 102:237–245.
6. Chaponnier, C., P. A. Janmey, and H. L. Yin. 1986. The actin filament-severing domain of plasma gelsolin. J. Cell Biol. 103:1473–1481.
7. Cooper, J. A. 1987. Effects of cytochalasin and phalloidin on actin. J. Cell Biol. 105:1473–1478.
8. Cooper, J. A., J. Bryan, B. Schwab III, C. Frieden, D. J. Loftus, and E. L. Elson. 1987. Microinjection of gelsolin into living cells. J. Cell Biol. 104:491–501.
9. Cooper, J. A., S. B. Walker, and T. D. Pollard. 1983. Pyrene actin: documentation of the validity of a sensitive assay for actin polymerization. J. Muscle Res. Cell Motil. 4:253–262.
10. Ey, P. L., and L. E. Ashman. 1986. The use of alkaline phosphatase-conjugated anti-immunoglobulin with immunoblots for determining specificity of monoclonal antibodies to protein mixtures. Meth. Enzym. 121:497–509.
11. Fujiwara, K. and T. D. Pollard. 1976. Fluorescent antibody localization of myosin in the cytoplasm, cleavage furrow and mitotic spindle of human cells. J. Cell Biol. 71:848–875.
12. Gibson, W. 1974. Polyoma virus proteins: a description of the structural proteins of the virion based on polyacrylamide gel electrophoresis and peptide analysis. Anal. Biochem. 62:319–336.
13. Hunkapiller, M. W., E. Lujan, F. Ostrander, and L. E. Hood. 1983. Isolation of microgram quantities of proteins from polyacrylamide gels for amino acid sequence analysis. Meth. Enzym. 91:227–236.
14. Hwo, S., and J. Bryan. 1986. Immunoidentification of Ca^{2+}-induced conformation changes in human gelsolin and brevin. J. Cell Biol. 102:227–236.
15. Jacobson, K., and J. Wojcieszyn. 1984. The translational mobility of substances within the cytoplasmic matrix. Proc. Natl. Acad. Sci. USA. 81:6747–6751.
16. Kwiatkowski, D. J., T. P. Stossel, S. H. Orkin, J. E. Mole, H. R. Colten, and H. L. Yin. 1986. Plasma and cytoplasmic gelsolins are encoded by a single gene and contain a duplicated actin-binding domain. Nature (Lond.). 323:455–458.
17. Nodes, B. R., J. E. Shackelford, and H. G. Lebherz. 1987. Synthesis and secretion of serum gelsolin by smooth muscle tissue. J. Biol. Chem. 262:5422–5427.
18. Pollard, T. D., and J. A. Cooper. 1982. Methods to characterize actin filament networks. Meth. Enzym. 85:316–321.
19. Pollard, T. D., and J. A. Cooper. 1986. Actin and actin-binding proteins. A critical evaluation of mechanisms and functions. Annu. Rev. Biochem. 55:987–1035.
20. Rouayrence, J. F., A. Fattoum, J. Gabrion, E. Audemard, and R. Kassab. 1984. Muscle Gelsolin—isolation from heart tissue and characterization as an integral myofibrillar protein. FEBS (Fed. Eur. Biol. Soc.) Lett. 167:52–58.
21. Sanger, J. W., B. Mittal, and J. M. Sanger. 1984. Interaction of fluorescently-labeled contractile proteins with the cytoskeleton in cell models. J. Cell Biol. 99:918–928.
22. Scott, R. E., R. G. Perkins, M. A. Zschunke, B. J. Hoerl, and P. B. Maercklein. 1979. Plasma membrane vesiculation in 3T3 and SV3T3 cells. I. Morphological and biochemical characterization. J. Cell Sci. 35:229–243.
23. Soua, Z., F. Porte, M.-C. Harricane, J. Feinberg, and J.-P. Capony. 1985.

Bovine serum brevin. Purification by hydrophobic chromatography and properties. *Eur. J. Biochem.* 153:275-287.

24. Stossel, T. P., C. Chaponnier, R. M. Ezzell et al. 1985. Nonmuscle actin-binding proteins. *Annu. Rev. Cell Biol.* 1:353-402.

25. Tank, D. W., E.-S. Wu, and W. W. Webb. 1982. Enhanced molecular diffusibility in muscle membrane blebs: release of lateral constraints. *J. Cell Biol.* 92:207-212.

26. Taylor, D. L., P. A. Amato, K. Luby-Phelps, and P. McNeil. 1984. Fluorescent analog cytochemistry. *Trends in Biochem. Sci.* 9:88-91.

27. Taylor, D. L., and Y.-L. Wang. 1980. Fluorescently labeled molecules as probes of the structure and function of living cells. *Nature (Lond.).* 284:405-410.

28. Towbin, H., T. Staehlin, and J. Gordon. 1979. Electrophoretic transfer of proteins from polyacrylamide gels to nitrocellulose sheets: procedure and some applications. *Proc. Natl. Acad. Sci. USA.* 76:4350-4354.

29. Wang, E., H. L. Yin, J. G. Krueger, L. A. Caliguiri, and I. Tamm. 1984. Unphosphorylated gelsolin is localized in regions of cell-substratum contact or attachment in Rous Sarcoma Virus-transformed rat cells. *J. Cell Biol.* 98:761-771.

30. Wang, Y.-L. 1986. Dynamics of filamentous actin in living non-muscle cells. *J. Cell Biol.* 103 (5, pt. 2):265a. Abstract.

31. Wu, E.-S., D. W. Tank, and W. W. Webb. 1982. Unconstrained lateral diffusion of concanavalin a receptors on bulbous lymphocytes. *Proc. Natl. Acad. Sci. USA.* 79:4962-4966.

32. Yin, H. L., J. H. Albrecht, and A. Fattoum. 1981. Identification of gelsolin, a Ca^{++}-dependent regulatory protein of actin gel-sol transformation and its intracellular distribution in a variety of cells and tissues. *J. Cell Biol.* 91:901-906.